Volume 24, No 3 | International Journal of Radiation Research, July 2026

Methionine deprivation enhances the radiosensitivity of glioma cells and promotes ionizing radiation-induced immunogenic cell death via the endoplasmic reticulum stress signaling pathway

S. Yang[1,2#], H. Qin[3#], X. Jiang[1], X. Xue[1], H. Tan[1], B. Wang[4], T. Sun[5], W. Yang[1*]

[1]*State Key Laboratory of Radiation Medicine and Protection, School of Radiation Medicine and Protection, Collaborative Innovation Center of Radiation Medicine of Jiangsu Higher Education Institutions, Soochow University, Suzhou, Jiangsu, China*

[2]*Radiological Health Assessment and Testing Center, Guangzhou Twelfth People's Hospital, Guangzhou, Guangdong, China*

[3]*Department of Thoracic Surgery, The First Affiliated Hospital of Soochow University, Suzhou, Jiangsu, China*

[4]*Department of Oncology, Second Affiliated Hospital of Soochow University, Suzhou, Jiangsu, China*

[5]*Neurosurgery and Brain and Nerve Research Laboratory, The First Affiliated Hospital of Soochow University, Suzhou, Jiangsu, China*

► ***Original article***

Corresponding author:
Wei Yang,
E-mail: *detachedy@aliyun.com*

Received: April 2025
Final revised: October 2025
Accepted: December 2025

Int. J. Radiat. Res., July 2026; 24(3): 627-639

DOI: 10.61186/ijrr.24.3.7

Keywords: *Methionine, glioma, autophagy, radiosensitivity, immunogenic cell death.*

#Shuangyu Yang and Hualong Qin contributed equally to the work.

ABSTRACT

Background: Methionine deprivation (MD) affects protein stability, signaling pathway activation and redox status of cancerous cells. In this study, we investigated the effects of MD on the radiosensitivity and radiation-induced immunogenic death of glioma cells and the underlying mechanism. ***Materials and Methods:*** Human glioma cells, U251 and T98G, were cultured in DMEM medium with or without methionine under normoxia or hypoxia (1% O_2). Cell proliferation, radiosensitivity, and DNA damage repair were detected by EdU assay, colony formation assay, γ-H2AX immunofluorescence staining and single-cell gel electrophoresis, respectively. Cell apoptosis and surface exposure of calreticulin (CRT) were detected via flow cytometry. The expression of autophagy-related proteins microtubule-associated protein 1 light chain 3 (LC3) and P62 and endoplasmic reticulum stress (ERS) pathway-related proteins PKR-like endoplasmic reticulum kinase (PERK) and inositol requiring enzyme 1 alpha (IRE1α) was detected via Western blotting. ***Results:*** MD inhibited the proliferation of normoxic or hypoxic glioma cells. MD combined with radiation promoted apoptosis and increased the number of γ-H2AX foci and the percentage of DNA in the tail of the comet. MD enhanced the radiosensitivity of normoxic or hypoxic glioma cells, which was further enhanced when combined with the autophagy inhibitor 3-methyladenine (3-MA). MD enhanced the transformation of LC3 I to LC3 II and decreased the expression of P62. MD also increased radiation-induced CRT exposure, ATP release and PERK and IRE1α phosphorylation. ***Conclusion:*** MD enhanced the radiosensitivity of glioma cells by inhibiting DNA repair and promoted ionizing radiation-induced immunogenic cell death through activating the ERS signaling pathway.

INTRODUCTION

Glioblastoma (GBM) is the most invasive and common primary malignant brain tumor [1]. Although standard treatments such as surgical resection, radiotherapy and chemotherapy are used [2], there is still no cure after GBM diagnosis, and the median survival time is only 15 months [3]. There are hypoxic regions in glioblastoma [4]. Hypoxia can mediate radiation resistance by reducing the degree of DNA damage [5]. Therefore, new methods for enhancing the efficacy of radiotherapy and chemotherapy are urgently needed.

Exogenous methionine (Met) is involved in a variety of metabolic processes, including the synthesis of polyamines and nucleotides, methylation and glutathione production. Methionine deprivation affects protein stability, phospholipid integrity, signaling pathway activation and redox status [6]. Methionine restriction (MR) or methionine deprivation (MD) can affect cancer progression. The deprivation of methionine, a cysteine donor, can result in the accumulation of reactive oxygen species (ROS) in glioma cells, leading to autophagy and the repression of proliferation [7]. The methionine cycle and folic acid cycle constitute two main components of one-carbon metabolism [6]. Metabonomic studies have revealed that interfering with one-carbon metabolism affects redox and nucleotide metabolism in tumor cells and that one-carbon metabolism has

[Downloaded from ijrr.com on 2026-08-16]

[DOI: 10.61186/ijrr.24.3.7]

become an intervention target [8], making MR/MD a new method for cancer treatment.

Autophagy is an adaptive response of cells to a variety of stresses. The cytoplasmic components that need to be degraded, including proteins, mitochondria and other organelles, are embedded in the double-layer membrane to form autophagosomes; then, they fuse with lysosomes to form autophagy lysosomes, and the components are degraded by lysosomal hydrolase [9]. Both MD and ionizing radiation (IR) can induce autophagy [7, 10].

Immunogenic cell death (ICD) is caused by chemical, physical, or infectious pathogens, and these factors trigger endoplasmic reticulum stress (ERs) mediated by ROS, resulting in stimulation of the immune system through the release or cell membrane surface exposure of damage-associated molecular patterns (DAMPs). The antitumor immune response is subsequently initiated [11]. DAMPs, including calreticulin (CRT), ATP [12], heat shock protein 70/90 (HSP70/90) [13], and high mobility group box 1 (HMGB1) [14], are very important for ICD. ICD is related to the activation of ERs signaling pathways, which regulate ER homeostasis or induce apoptosis through three ERs receptors, PKR-like endoplasmic reticulum kinase (PERK), inositol requiring enzyme 1 alpha (IRE1α) and activating transcription factor 6 (ATF6) [15].

In this study, the effects and mechanism of MD on the radiosensitivity and IR-induced ICD of human glioma U251 and T98G cells were detected under normoxia and hypoxia. Unlike existing studies that have focused on the effects of MD on tumor cells under normoxia, this study investigated the changes in the glioma phenotype, radiosensitivity, autophagy, and ICD and ERs pathway activation under normoxia and hypoxia, offering a novel perspective by comparing the effects of normoxia with those of the hypoxic effects of MD. In addition, this study provided the first in-depth exploration of the synergistic effects of combining MD with an autophagy inhibitor on radiosensitivity and ICD, thereby introducing new combination therapeutic strategies to improve the effectiveness of glioma radiotherapy.

MATERIALS AND METHODS

Cell culture

Two typical human glioma cell lines, U251 and T98G, were cultured in DMEM (L110KJ, BasalMedia Technologies Co., Ltd., Shanghai, China) or methionine deprivation medium containing 10% fetal bovine serum (04-010-1A, BI, Israel) and 1% streptomycin and penicillin (Beyotime, Shanghai, China). Methionine deprivation medium was made by adding filtered L-cystine, hydrochloride (1:2) (30925 -07-6; Macklin Biochemical Co., Ltd., Shanghai, China), L-glutamine (25030081; Invitrogen, USA) and sodium pyruvate (11360070; Invitrogen, USA) to DMEM (21013-024; Invitrogen, USA). The autophagy inhibitor 3-Methyladenine (3-MA, 5 mM final concentration, 5142-23-4; InvivoGen, San Diego, USA) was added to the culture medium when needed. All the cells were cultured at 37°C, 5% CO2 and a certain humidity. The cells subjected to hypoxia were cultured in a hypoxia workstation (Invivo2 1000, Ruskinn, UK) with 1% O_2, 5% CO_2, and 94% N_2.

Radiation treatment

The cells were irradiated with 8 Gy X-ray (160 kV, 25 mA, 1.225 Gy/min) via a biological X-ray irradiator (RS-2000 Pro, Rad source, USA).

EdU staining assay

The cell proliferation rates were detected with an EdU-488 cell proliferation detection kit (C0071L, Beyotime, Shanghai, China). The cells were incubated with 500 μL of 5-ethynyl-2'-deoxyuridine (EdU) at 37°C for 2 h, fixed with 4% paraformaldehyde at room temperature for 15 min, permeabilized for 15 min with PBS containing 0.3% Triton X-100, and incubated for 30 min with 500 μL of Click reaction solution in the dark. The cells were stained with Hoechst 33342 for 10 min and detected via fluorescence microscopy (IX73, Olympus, Japan). The ratio of EdU-positive cells (green) to Hoechst-positive cells (blue) represented the cell proliferation rate.

Scratch assay

The cells were seeded in a plate with a diameter of 60 mm and treated accordingly. A sterile 200 μL pipette tip was used to make a single scratch, after which the cells were incubated in culture medium without FBS. The cells in the irradiation group were irradiated with 8 Gy X-rays. The scratch images were obtained via fluorescence microscopy (IX73, Olympus, Japan) at 0, 24 and 48 h after irradiation, and the scratch area was analyzed via ImageJ.

Immunofluorescence staining

The cells (5×10^5) were seeded in a plate with a diameter of 35 mm covered with chamber slides. After the cells had adhered to the wall, 8 Gy X-rays were given. At 0 h, 0.5 h, 1 h, 2 h, 4 h and 12 h after irradiation, the cells were fixed with 4% paraformaldehyde at room temperature for 15 min, permeabilized with 3% Triton X-100 in PBS for 15 min, blocked with immunostaining blocking solution for 45 min, incubated with a rabbit anti-γ-H2AX monoclonal antibody (1:1000, ab81299, Abcam, UK) overnight at 4°C, washed with PBS three times, and incubated with an Alexa Fluor 555-conjugated donkey anti-rabbit secondary antibody (1:500, A0453, Beyotime, Shanghai, China) for 45 min at room temperature. The nuclei were stained with Hoechst 33342 for 10 min, and the number of γ-H2AX focal points in the nuclei was measured with a

[Downloaded from ijrr.com on 2026-08-16]

[DOI: 10.61186/ijrr.24.3.7]

confocal laser-scanning microscope (FV1200, Olympus, Japan). For each coverslip, three to five tile areas were imaged. At least 500 cells were evaluated per sample per staining. DNA damage foci were analyzed via ImageJ. The total number of γ-H2AX foci was determined by local fluorescence maxima within the nucleus.

Single-cell gel electrophoresis (Comet assay)

Ten microliters of cell suspension (1×10^5 cells) were mixed with 40 μL of 1% LMA agarose (Biosharp, Beijing, China) at 0.5 h, 1 h, 2 h, 4 h and 12 h after irradiation and placed onto slides. The slide was submerged in neutral lysis solution at 37°C for 1 h in the dark (the lysis solution was precooled above 20 min at 4°C) and then soaked at 4°C in electrophoretic buffer for 30 min. After incubation, electrophoresis was run for 40 min at 23 V. The cells were immersed in the DNA precipitant at room temperature for 30 min and then soaked in 70% ethanol for 30 min. After the sample was dried, it was immersed and stained in SYBR Green I diluent (1:10000) for 30 min at room temperature. The images were observed and recorded under a confocal laser-scanning microscope (FV1200, Olympus, Japan). The percentage of DNA in the tail of the comet was determined by the comet score.

Colony formation assay

The cells were cultured in 6-well plates and given different doses of IR. After two weeks of culture, the cells were fixed with 4% paraformaldehyde (P0099, Beyotime, Shanghai, China) for 15 min and stained with crystal violet (C0121, Beyotime, Shanghai, China) for 30 min. The numbers of clones with more than 50 cells were observed and counted via fluorescence microscopy. The colony formation rate and the surviving fraction were subsequently calculated, and the mean lethal dose (D_0) was calculated via a linear quadratic model. The sensitivity enhancement ratio (SER) was calculated as a ratio of D_0, and the oxygen enhancement ratio (OER) was calculated as hypoxic D_0/normoxic D_0. The other two radiobiological parameters, the number of targets per cell (N) and the quasi-threshold dose (Dq), were also calculated.

Transmission electron microscopy (TEM)

The cells were harvested, and 1 mL of 2.5% (EM grade) glutaraldehyde (P1126, Solarbio, Beijing, China) was added. The volume ratio of glutaraldehyde to cells should be greater than 10:1. The cells were picked gently, suspended in glutaraldehyde, fixed for 30 min in the dark at room temperature, and then transferred to 4°C for storage. The glutaraldehyde should not freeze. The samples were transported in 4°C ice bags for inspection, and the glutaraldehyde did not freeze during transportation.

Flow cytometric analysis of apoptosis and cell cycle distribution

The rate of apoptosis was detected with an Annexin V-PE/7-AAD apoptosis kit (AT104, Multi Sciences, Zhejiang, China). The cells (4×10^5 cells/well) were collected, 5 μL of Annexin V-PE and 10 μL of 7-AAD were added, and the cells were incubated at room temperature in the dark for 5 min. Then, 400 μL of 1×binding buffer was added to resuspend the cells, and apoptosis was analyzed via flow cytometry (FACS Verse, BD, USA). The cell cycle distribution was detected via a cell cycle staining kit. The cells (4×10^5 cells/well) were collected, fixed, hydrated, added to 400 μL of DNA staining solution and incubated at room temperature in the dark for 30 min. The cell cycle distribution was analyzed via flow cytometry (FACS Verse, BD, USA).

Flow cytometry analysis of CRT surface exposure

The cells (3×10^5 cells/well) were harvested, PE-conjugated anti-calreticulin antibodies (1:50, 19780s, CST, USA) were added, and the cells were incubated for 30 min in the dark on ice. The cells were washed with PBS three times, 300 μL of 1× binding buffer was added, 5 μL of FITC Annexin V and 5 μL of 7-AAD (640922, Biolegend, USA) were added, and the mixture was incubated in the dark for 10 min. The positive rate of CRT on the cell membrane was detected via flow cytometry.

Extracellular ATP levels

The ATP standard solution and ATP detection working solution were prepared according to the instructions of the ATP assay kit (S0026, Beyotime, Shanghai, China). The cell supernatants were collected, and 100 μL of the ATP detection working solution was added to each well in the dark. Then, 100 μL of the sample or standard was added, mixed quickly, and incubated for 2–3 seconds. The luminescence value was detected with a microplate reader.

Western blot

The cells were harvested, washed with PBS 3 times and lysed on ice for 45 min. The protein samples were loaded and separated via SDS–PAGE and then transferred onto polyvinylidene fluoride (PVDF) membranes. The blots were incubated with primary antibodies against P62 (1:10000, ab109012, Abcam, UK), LC3B (1:2000, ab192890, Abcam, UK), PERK (1:1000, ab229912, Abcam, UK), p-PERK (1:1000, AF5902, Beyotime, Shanghai, China), IRE1α (1:1000, 3294, CST, USA), p-IRE1α (1:1000, ab243665, Abcam, UK), and β-actin (1:1000, AA128, Beyotime, Shanghai, China) at 4°C and incubated with HRP-conjugated secondary antibodies at room temperature for 1 hour. Specific proteins were visualized with enhanced chemiluminescence (ECL, P2300, NCM Biotech, Suzhou, China).

[Downloaded from ijrr.com on 2026-08-16]

[DOI: 10.61186/ijrr.24.3.7]

Statistical analysis

All the data were presented as the means ± standard deviations (SDs) of three independent experiments. GraphPad Prism 8 software (GraphPad Software, Boston, USA) was used for the statistical analyses. Differences in means were considered statistically significant at P<0.05. Student's t test was used for comparisons of data between two groups. For comparisons among more than two groups, one-way analysis of variance (ANOVA) followed by the Bonferroni post hoc correction was performed.

RESULTS

MD inhibited glioma cell proliferation

To explore the effect of methionine deprivation on the proliferation of GBM cells, an EdU cell proliferation experiment was carried out. Compared with met (+) conditions, met (-) conditions significantly inhibited the proliferation of glioma cells (figure 1 A-D). The cell proliferation rate of the hypoxia group was lower than that of the normoxia group. These results indicated that MD inhibited the proliferation of glioma cells, especially under hypoxia.

MD altered the cell cycle distribution of glioma cells

What is the effect of methionine deprivation on the cell cycle progression of glioma cells? After the cells were cultured under normoxic and hypoxic conditions for 24 hours, cell cycle progression was detected by flow cytometry. The results revealed that the proportion of cells in the G0/G1 phase in the met (-) group was significantly greater than that in the met (+) group under normoxia or hypoxia, whereas the proportion of cells in the S and G2/M phases was lower. Twenty-four hours after 8 Gy X-ray irradiation, the proportion of cells in the G0/G1 phase in the met (-) group was greater than that in the met (+) group under normoxia or hypoxia (figure 1 E-F). The above results suggested that MD changed the cycle distribution of glioma cells with or without irradiation.

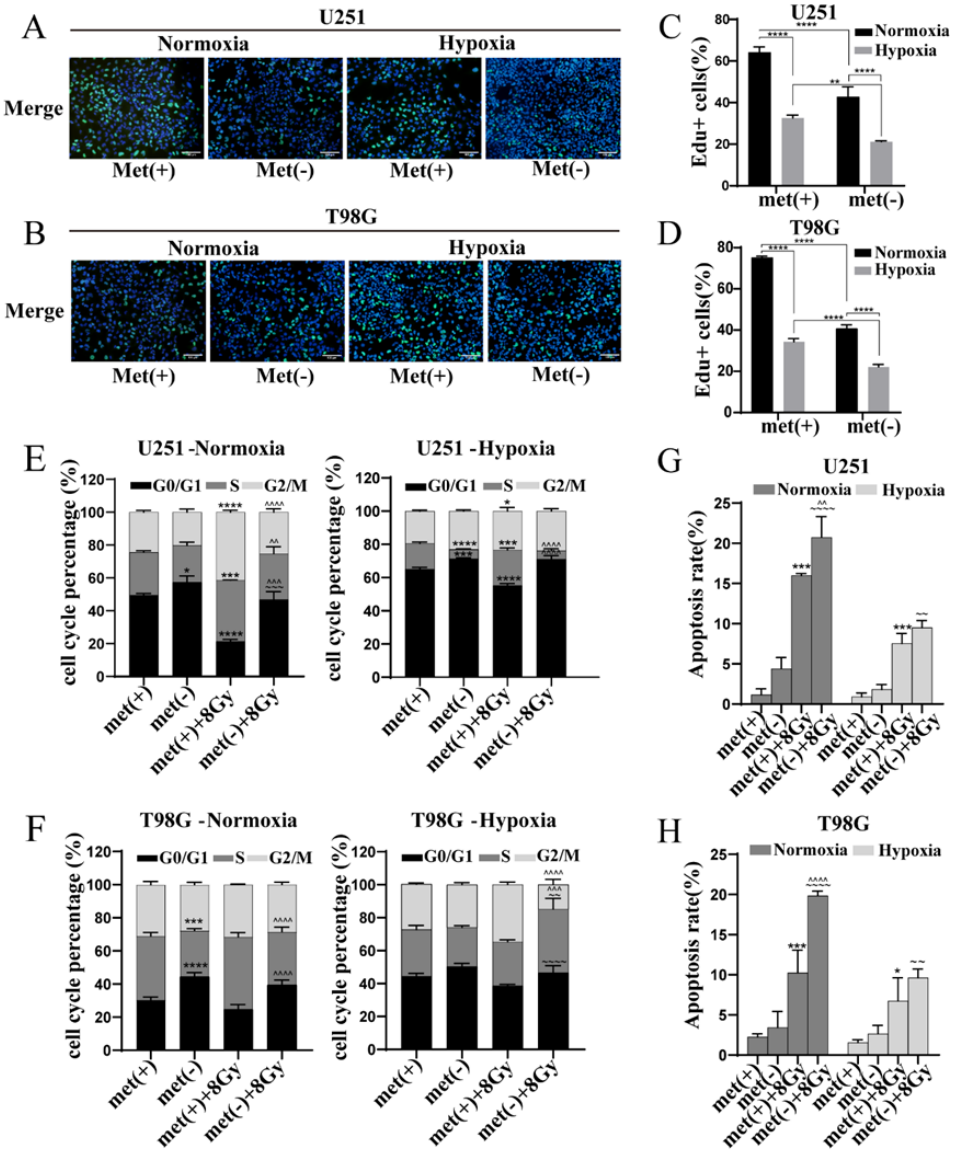

Figure 1. Methionine deprivation inhibited cell proliferation and enhanced irradiation-induced cell cycle arrest and apoptosis. **(A-D)** Glioma cells were cultured in DMEM or DMEM with methionine deprivation for 48 h. Then, the cells were stained with Azide Alexa Fluor 488 (green) to detect EdU, and the nuclei were stained with Hoechst 33342 (blue). Scale bar: 100 μm. **(E-F)** Cell cycle profiles obtained via PI staining via flow cytometry. The data are presented as percentages of glioma cells in G0/G1, S and G2/M at 24 h after irradiation. **(G-H)** Flow cytometric analysis of Annexin V-PE and 7-AAD staining for the determination of apoptosis in glioma cells after irradiation for 24 h. * P < 0.05, ** P < 0.01, *** P < 0.001 and **** P < 0.0001 compared to met (+). ~ P < 0.05, ~ ~ P < 0.01, ~ ~ ~P < 0.001 and ~ ~ ~ ~P < 0.0001 compared to met (-). ^ P < 0.05, ^ ^P < 0.01, ^^^ P < 0.001 and ^^^^ P < 0.0001 compared to met (+)+8 Gy.

[Downloaded from ijrr.com on 2026-08-16]

[DOI: 10.61186/ijrr.24.3.7]

MD enhanced the IR-induced apoptosis of normoxic glioma cells

To explore the effect of MD on the apoptosis of GBM cells, flow cytometry was used to detect the effects of MD and/or X-ray irradiation on the apoptosis of glioma cells. Under normoxic or hypoxic conditions, the total apoptosis rate of met (-) cells was greater than that of met (+) cells, but the difference was not significant. Under normoxia, the total apoptosis rate of glioma cells in the met (-) + 8 Gy group was significantly greater than that in the met (+) + 8 Gy group at 24 h after 8 Gy X-ray irradiation. Under hypoxia, the total percentage of apoptotic cells in the met (-) + 8 Gy group was greater than that in the met (+) + 8 Gy group, but the difference was not significant (figure 1 G-H). These results showed that MD enhanced the IR-induced apoptosis of normoxic glioma cells.

MD inhibited the migration of glioma cells

To explore the effect of MD on the migration of glioma cells, a scratch assay was carried out. Under normoxic and hypoxic conditions, the mobility of met (-) cells was lower than that of met (+) cells at 24 h and 48 h. The migration rate of the met (-) + 8 Gy group was lower than that of the met (+) + 8 Gy group at 24 h and 48 h. In addition, the migration rate of the irradiated group was lower than that of the non -irradiated group (figure 2 A-B). These results suggested that MD inhibited the migration of normoxic or hypoxic glioma cells.

MD aggravated IR-induced DNA double-strand breaks in glioma cells

In the immunofluorescence assay, the effect of MD on the degree of DNA damage in glioma cells after irradiation was determined by detecting the number of γ-H2AX foci. Under normoxic and hypoxic conditions, the number of γ-H2AX foci in met (-) cells was greater than that in met (+) cells, but the difference was not significant. Glioma cells were irradiated with 8 Gy X-ray. The number of γ-H2AX foci in the met (-) group was greater than that in the met (+) group at 0.5 h, 1 h, 2 h and 4 h after irradiation, indicating that DNA damage was more severe in the met (-) group. The number of γ-H2AX foci was the highest at 1 h after irradiation. Over time, the damage was gradually repaired after irradiation (figure 2 C-E).

In the single-cell gel electrophoresis assay, the percentage of DNA in the tail was detected to determine the effect of MD on the degree of DNA damage in glioma cells after irradiation. The experimental results were essentially consistent with the above results of the immunofluorescence assay. Under normoxic and hypoxic conditions, the percentage of DNA in the tail of met (-) cells was greater than that in met (+) cells, but the difference was not significant. The percentage of DNA in the tails of met (-) cells was significantly greater than that in the tails of met (+) cells at 0.5 h, 1 h and 4 h after 8 Gy X-ray irradiation (figure 2 F-H). These results suggested that MD aggravated IR-induced DNA double-strand breaks (DSBs) in normoxic or hypoxic glioma cells.

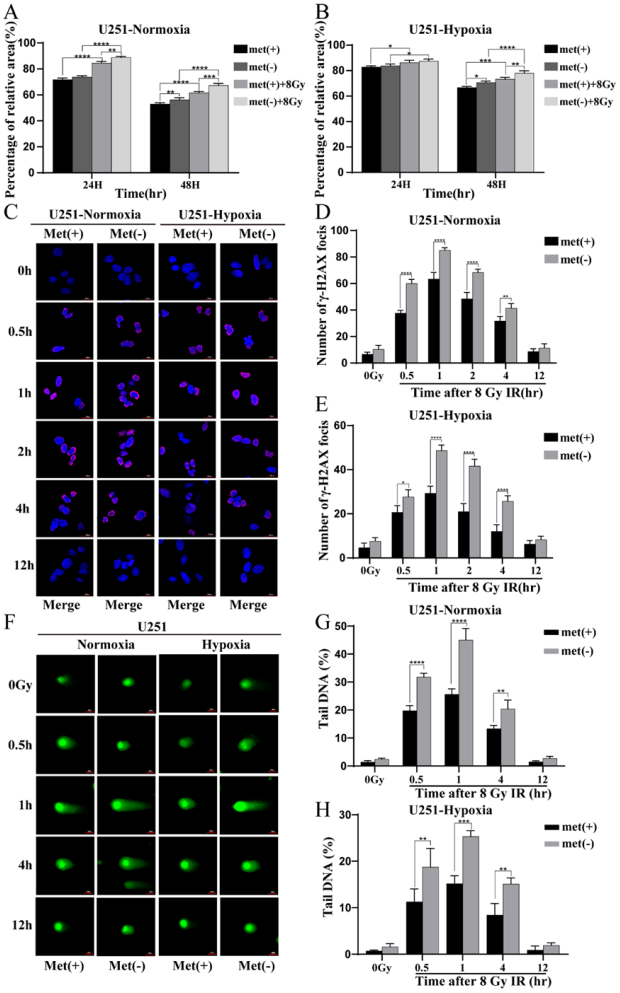

Figure 2. Methionine deprivation inhibited cell migration and aggravated IR-induced DNA damage. **(A-B)** Methionine deprivation promoted glioma cell migration, as analyzed by a cell scratch assay. Scale bar: 200 μm. **(C-E)** Immunofluorescence staining of γ-H2AX after 8 Gy irradiation in glioma cells. Scale bar: 20 μm. **(F-H)** DNA damage at various time points after 8 Gy irradiation was assessed via single-cell gel electrophoresis under neutral conditions (neutral comet assay). Scale bar: 20 μm. The data are presented as the means ± SDs. *p < 0.05, ** p < 0.01, *** p < 0.001, **** p < 0.0001.

MD enhanced the radiosensitivity of glioma cells

A clonal survival assay was used to detect whether MD affects the radiosensitivity of glioma cells. Under normoxic and hypoxic conditions, the sensitivity enhancement ratios (SERs) of met (-) for U251 cells were 1.518 and 1.554, respectively, and the oxygen enhancement ratios (OERs) of met (+) and met (-) were 2.134 and 2.084, respectively (figure 3A). These SER data indicated that MD enhanced the radiosensitivity of glioma cells under normoxia or hypoxia.

[Downloaded from ijrr.com on 2026-08-16]

[DOI: 10.61186/ijrr.24.3.7]

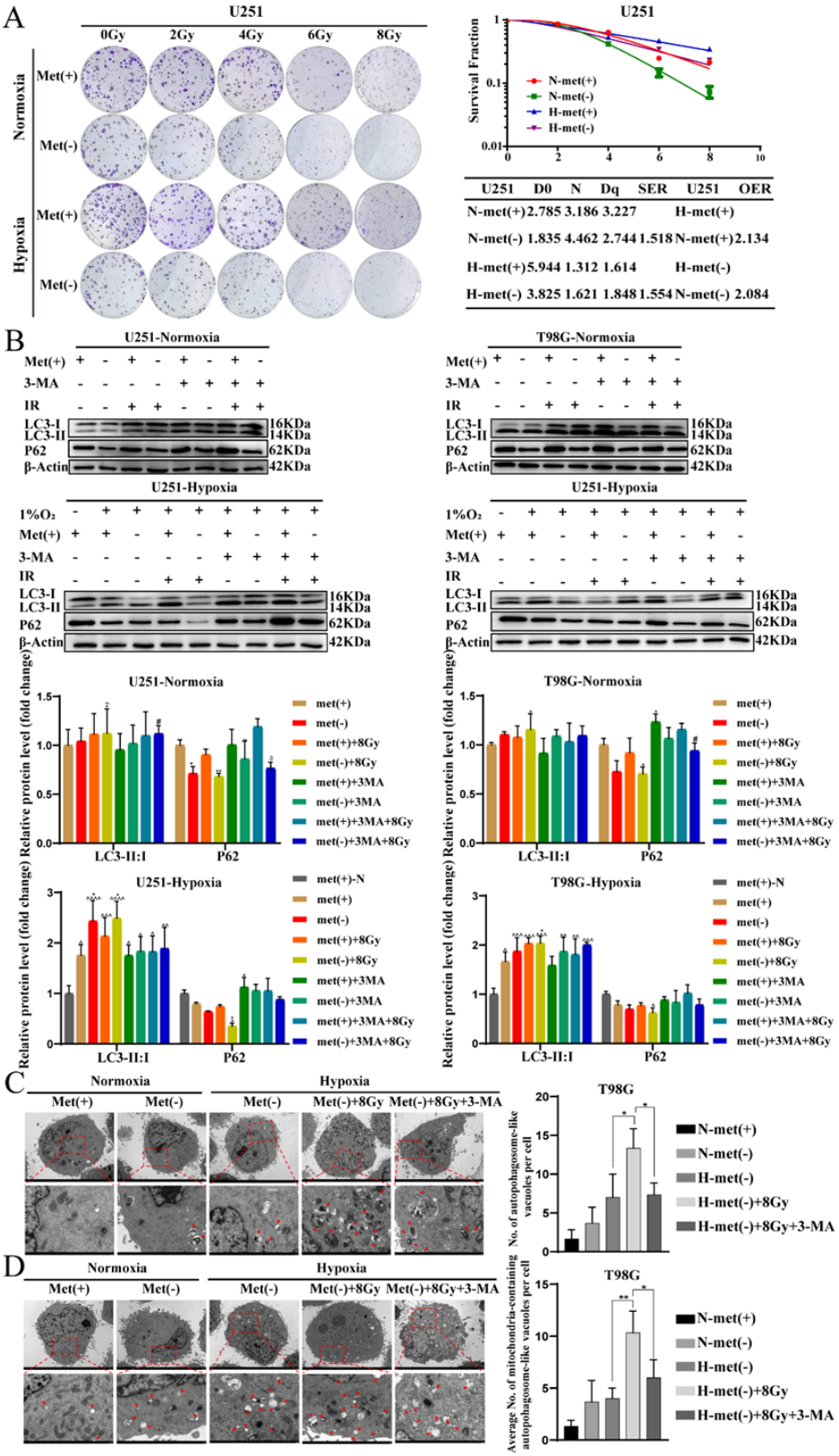

Figure 3. Methionine deprivation enhanced the radiosensitivity of irradiation-induced glioma cells, upregulated the expression of LC3-II, downregulated the expression of P62, and promoted autophagy and mitophagy. **(A)** The relative colony formation rate of glioma cells after methionine deprivation under normoxia and hypoxia was measured via a colony formation assay. **(B)** Western blot analysis was presented for LC3B-I/II and P62 levels, with a β-actin loading control. **(C)** Autophagy in cells was photographed via TEM. **(D)** The engulfment of mitochondria in autophago-some-like vacuoles in glioma cells, as shown by TEM-based ultrastructure analyses. Red arrowheads indicate autophagosome-like vacuoles. Scale bar for original images, 5 μm; scale bar for enlarged images, 1 μm. The data are presented as the means ± SDs. ^P<0.05, ^^P<0.01, ^^^P<0.001, ^^^^P<0.0001 compared with met(+)-N. *P<0.05, **P<0.01, ***P<0.001, ****P<0.0001 compared with met(+). #P<0.05, ##P<0.01, ###P<0.001, ####P<0.0001 compared with the met(+)+3-MA group. ~P<0.05, ~~P<0.01, ~~~P<0.001, ~~~~P<0.0001 compared with met(-). &P<0.05, &&P<0.01, &&&P<0.001, &&&&P<0.0001 compared with met(-)+3-MA.

MD upregulated LC3-II expression and downregulated P62 expression in irradiated glioma cells

The expression of the autophagy-associated proteins LC3-II and P62 was detected by Western blotting. Compared with the control, MD alone induced the transformation of the autophagy-related protein LC3-I to LC3-II and decreased the expression of P62 in glioma cells. Compared with those in the nonirradiated group, LC3-II expression was increased, and P62 expression was decreased in the 8 Gy irradiation group. Compared with 8 Gy irradiation alone, MD combined with 8 Gy irradiation aggravated autophagy, increased the expression of LC3-II and

[Downloaded from ijrr.com on 2026-08-16]

[DOI: 10.61186/ijrr.24.3.7]

decreased the expression of P62. Similarly, compared with irradiation combined with 3-MA, MD combined with irradiation and 3-MA increased LC3-II expression and decreased P62 expression (figure 3 B).

MD increased IR-induced autophagosome formation and mitophagy in glioma cells

To study the effect of MD on irradiation-induced autophagy in glioma cells, the cellular ultrastructure was observed via transmission electron microscopy (TEM). MD increased the formation of autophagosomes and the engulfment of mitochondria in autophagosome-like vacuoles in T98G cells under normoxic and hypoxic conditions, but the differences were not significant. Under hypoxic conditions, MD significantly increased the formation of IR-induced autophagosomes in glioma cells. Mitochondria are the main oxygen-consuming organelles in mammalian cells. Hypoxia can induce mitochondrial fission, thus promoting mitochondrial turnover through autophagy to limit cell oxygen consumption. TEM revealed that, compared with irradiation alone, MD combined with irradiation increased the engulfment of mitochondria in autophagosome-like vacuoles in glioma cells under hypoxia. The autophagy-dependent clearance of mitochondria reduced oxygen consumption, made cells resistant to hypoxia and maintained cell viability. In contrast, the autophagy inhibitor 3-MA inhibited the formation of autophagosomes and the engulfment of mitochondria in autophagosome-like vacuoles in glioma cells (figure 3 C-D).

Autophagy inhibition promoted MD- and IR-induced glioma apoptosis

Previous experimental results showed that MD enhanced irradiation-induced glioma apoptosis. Since MD increased IR-induced autophagy, we hypothesized that autophagy inhibition might promote MD- and IR-induced glioma apoptosis. The percentage of apoptosis in each group was detected via flow cytometry. Under normoxic and hypoxic conditions, regardless of the presence of MD, the apoptosis rate of the 3-MA group was greater than that of the non-3-MA group, indicating that the inhibition of autophagy promoted glioma apoptosis and that autophagy exerted a protective effect in this context. Under normoxia, the apoptosis rate of glioma cells in the met (-) + 3-MA group was significantly greater than that in the met (+) + 3-MA group. The percentage of apoptotic cells in the met (-) + 8 Gy+ 3-MA group was significantly greater than that in the met (+) +8 Gy + 3-MA group. Under hypoxia, the apoptosis rate of glioma cells in the met (-) + 3-MA group was greater than that in the met (+) + 3-MA group, and the apoptosis rate of the met (-) + 8 Gy + 3 -MA group was significantly greater than that of the met (+) + 8 Gy + 3-MA group (figure 4 A-D).

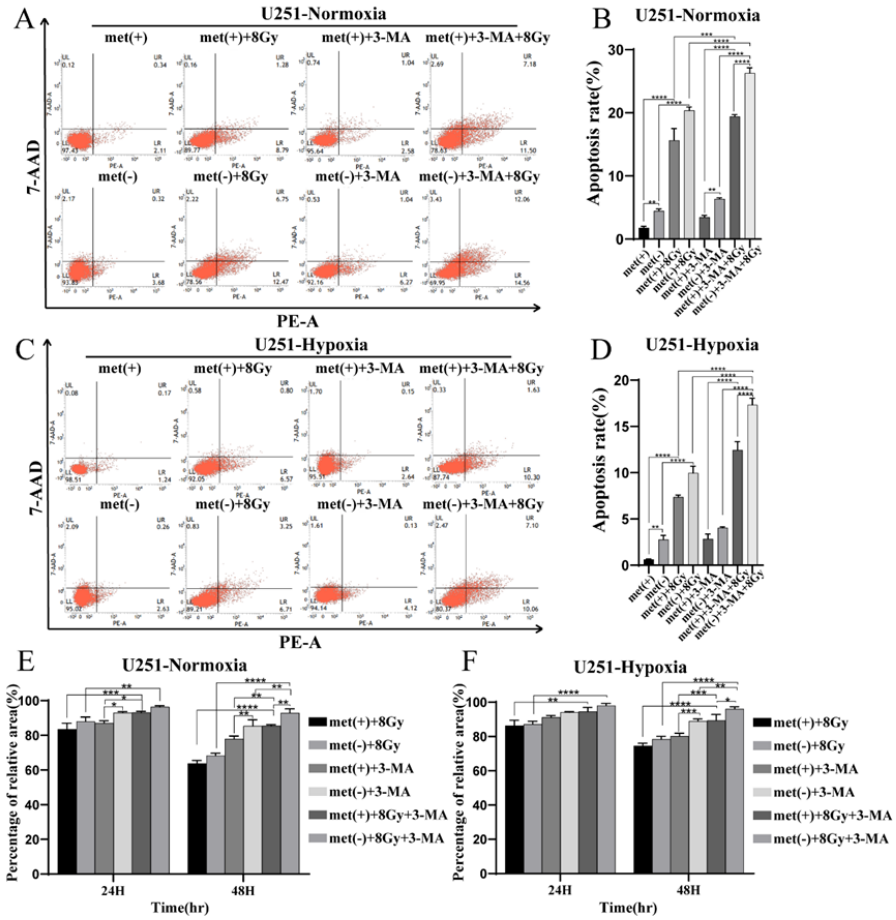

Figure 4. Methionine deprivation combined with 3-MA further enhanced irradiation-induced apoptosis and inhibited cell migration. **(A-D)** After methionine deprivation combined with 3-MA and 8 Gy treatment, the apoptosis rate of glioma cells after 24 h of irradiation was detected via flow cytometry analysis of Annexin V-PE and 7-AAD staining. **(E-F)** After methionine deprivation combined with 3-MA and 8 Gy treatment, the cell scratch assay revealed that methionine combined with 3-MA promoted IR-induced glioma cell migration. Scale bar: 200 μm. The data are presented as the means ± SDs. *p < 0.05, ** p < 0.01, *** p < 0.001, **** p < 0.0001.

[Downloaded from ijrr.com on 2026-08-16]

[DOI: 10.61186/ijrr.24.3.7]

MD combined with 3-MA further inhibited glioma cell migration

Cell migration was observed by fluorescence microscopy and quantitatively analyzed. The cell migration rate of the 3-MA combined with IR group was significantly lower than that of the IR group at 24 h and 48 h after irradiation, suggesting that the autophagy inhibitor 3-MA inhibited the migration of glioma cells. Under normoxic and hypoxic conditions, the cell migration rate of the met (-) + 3-MA group was lower than that of the met (+) + 3-MA group. In addition, the cell migration rate of the met (-) + 8 Gy + 3-MA group was lower than that of the met (+) + 8 Gy + 3-MA group, suggesting that MD combined with autophagy inhibition further inhibited glioma cell migration (figure 4 E-F).

MD combined with 3-MA further aggravated IR-induced DNA double-strand breaks in glioma cells

The dynamic changes in DNA DSBs in normoxic and hypoxic glioma cells at different time points after X-ray irradiation were detected via γ-H2AX immunofluorescence staining. After glioma cells were treated with 3-MA and irradiated with 8 Gy X-rays, the number of γ-H2AX foci in the met (-) + 3-MA group was significantly greater than that in the met (+) + 3-MA group at 0.5 h, 1 h, 2 h and 4 h after irradiation. The number of γ-H2AX foci reached a maximum at 1 h after irradiation and then decreased with time, and the damage was repaired gradually at 12 h after irradiation. The number of γ-H2AX foci in glioma cells treated with MD combined with 3-MA was significantly greater than that in cells treated with MD at different time points after irradiation. The above experimental data suggested that compared with MD alone or 3-MA alone, MD combined with 3-MA can significantly aggravate radiation-induced DSBs in normoxic or hypoxic glioma cells (figure 5A-D).

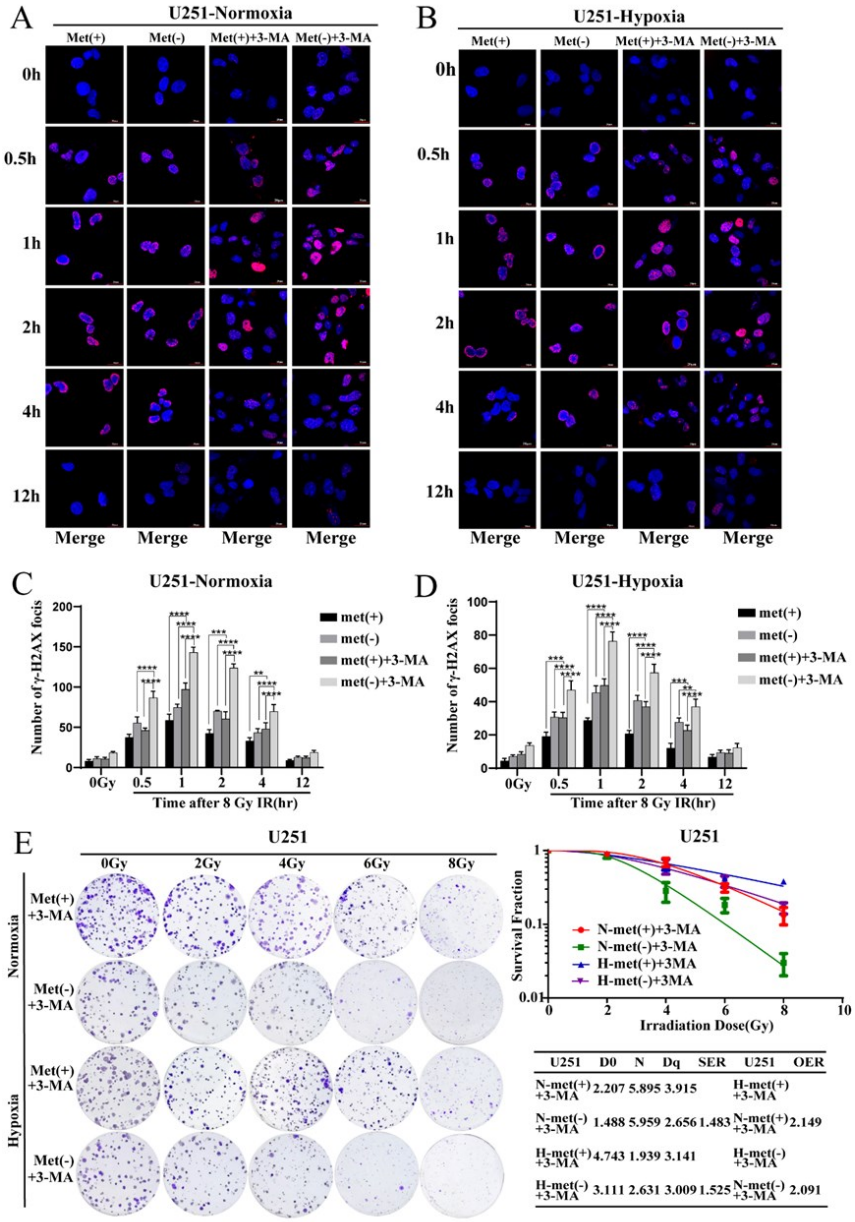

Figure 5. Methionine deprivation combined with 3-MA further aggravated irradiation-induced DNA damage and significantly enhanced the radiosensitivity of GBM. **(A-D)** After methionine deprivation combined with 3-MA and 8 Gy treatment, immunofluorescence staining of γ-H2AX in glioma cells was performed. Scale bar: 20 μm. **(E)** The relative colony formation rate of glioma cells after treatment with methionine deprivation combined with 3-MA under normoxia and hypoxia was measured via a colony formation assay. *p < 0.05, ** p < 0.01, *** p < 0.001, **** p < 0.0001.

[Downloaded from ijrr.com on 2026-08-16]

[DOI: 10.61186/ijrr.24.3.7]

MD combined with 3-MA further enhanced the radiosensitivity of glioma cells

Colony formation assays were used to explore variations in radiobiological parameters (D_0, D_q, N, SER and OER). For normoxic or hypoxic U251 cells, the SERs of the met (-) + 3-MA group were 1.483 and 1.525, respectively, compared with those of the met (+) + 3-MA group. The above SER values suggested that MD increased the radiosensitivity of normoxic and hypoxic glioma cells treated with the autophagy inhibitor 3-MA (figure 5E). According to the D_0 values (figure 5E and 3A), the SER of U251 cells in the N-met (+) + 3-MA group compared with the N-met (+) group was 1.262. The SER of U251 cells in the N-met (-) + 3-MA group compared with the N-met (-) group was 1.233. The SER of U251 cells in the H-met (+) + 3-MA group compared with the H-met (+) group was 1.253. The SER of U251 cells in the H-met (-) + 3-MA group compared with the H-met (-) group was 1.230. These results suggested that MD combined with an autophagy inhibitor significantly increased the radiosensitivity of normoxic or hypoxic glioma cells compared with MD alone or 3-MA alone.

MD enhanced IR-induced cell membrane surface exposure of CRT

Flow cytometry was used to detect CRT exposure on the cell membrane surface of U251 and T98G cells. At 4 h and 24 h after irradiation, the exposure of CRT on the surface of glioma cells in the MD combined with IR group was greater than that in the IR group, suggesting that MD increased IR-induced CRT membrane exposure, which was most obvious at 24 h after irradiation. Nevertheless, 3-MA attenuated MD- and/or IR-induced CRT exposure (figure 6 A-B).

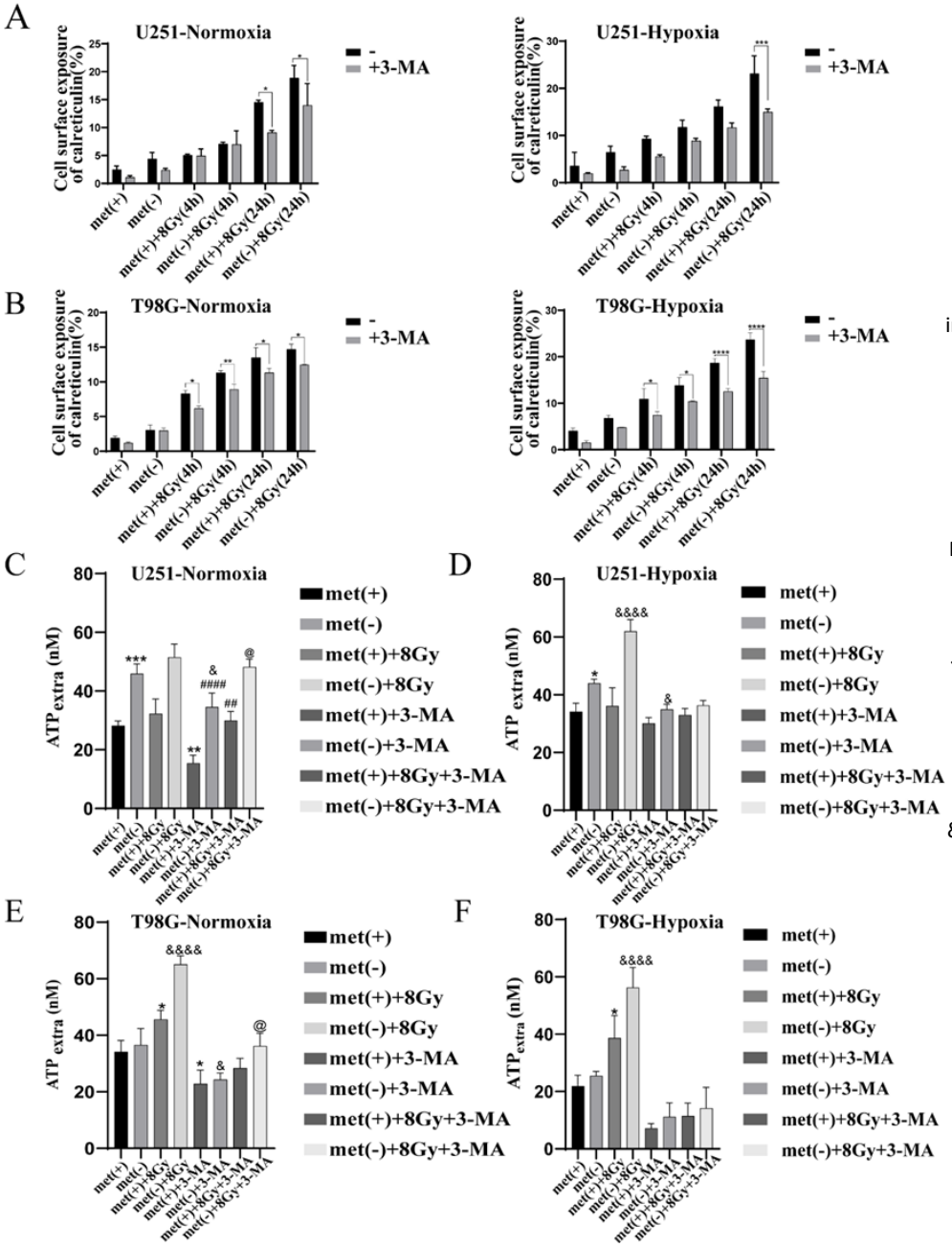

Figure 6. Methionine deprivation enhanced irradiation-induced membrane exposure of CRT cells and promoted the release of ATP in the cell supernatant. **(A-B)** CRT exposure on the surface of the cell membrane under normoxia and hypoxia. * P<0.05, ** P<0.01, *** P<0.001, **** P<0.0001. **(C-F)** Release of ATP from the cell supernatant of cells under normoxia and hypoxia. *P <0.05, **P<0.01, ***P<0.001, ****P<0.0001 compared to met (+); #P<0.05, ##P<0.01, ###P<0.001, ####P <0.0001 compared to met (+)+3-MA; &P<0.05, &&P<0.01, &&&P<0.001, &&&&P<0.0001 compared to met (-); @P<0.05, @@P<0.01, @@@P<0.001, @@@@P<0.0001 compared to met (-)+3-MA.

[Downloaded from ijrr.com on 2026-08-16]

[DOI: 10.61186/ijrr.24.3.7]

MD enhanced IR-induced ATP release in the supernatants of glioma cells

To explore the effects of MD and/or 3-MA on the IR-induced release of DAMPs, ATP release in the supernatants of U251 and T98G glioma cells was detected via a biochemical luminescence assay. Compared with that in the control group, the ATP content in the supernatant of glioma cells in the MD group was significantly greater at 24 h after irradiation. Similarly, compared with 3-MA, MD combined with 3-MA increased the release of ATP at 24 h after irradiation. Compared with the IR + 3-MA group, the MD + IR + 3-MA group exhibited increased ATP release. Nevertheless, 3-MA attenuated MD- and/or IR-induced ATP release. These results suggested that MD could increase IR-induced ATP release and that autophagy inhibition could attenuate ATP release (figure 6 C-F).

MD enhanced the IR-induced phosphorylation of ERs related PERK and IRE1α proteins in glioma cells

The above results showed that MD enhanced the ICD of normoxic and hypoxic glioma cells induced by IR and that the inhibition of autophagy reduced the occurrence of ICD and the exposure or release of DAMPs. To further explore this mechanism, the expression of ERs related proteins PERK, p-PERK, IRE1α and p-IRE1α was detected via Western blotting. Under both normoxic and hypoxic conditions, there was no significant change in the protein expression of PERK and IRE1α in glioma cells (figure 7 A-B). Under normoxic and hypoxic conditions, the levels of p-PERK and p-IRE1α in U251 and T98G cells in the MD group were greater than those in the control group. Compared with those in the IR group, the protein levels of p-PERK and p-IRE1α in glioma cells in the MD + IR group were significantly greater. Compared with those in the 3-MA group, the phosphorylation levels of PERK and IER1α in the MD + 3-MA group were greater. Compared with those in the 3-MA + IR group, the protein levels of p-PERK and p-IER1α in the MD + 3-MA+ IR group were significantly greater. Nevertheless, 3-MA attenuated MD- and/or IR-induced p-PERK and p-IER1α protein expression. These results suggested that MD and IR induced ICD through the activation of ERs signaling pathways.

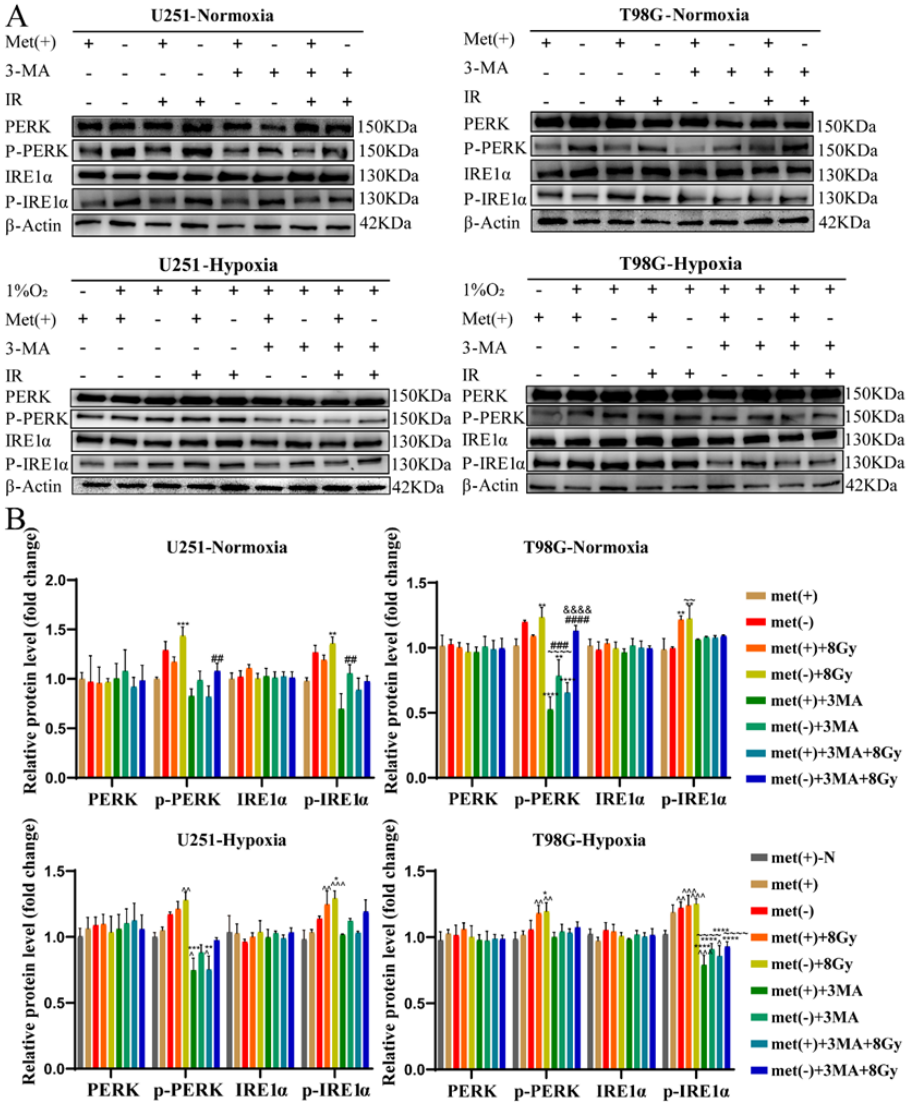

Figure 7. Methionine deprivation and ionizing radiation increased the level of phosphorylation of PERK and IRE1α in ERs-related pathways. **(A-B)** Western blot analysis results are presented for PERK, IRE1α, p-PERK and p-IRE1α levels, with a β-actin loading control. ^P<0.05, ^^P<0.01, ^^^P<0.001, and ^^^^P<0.0001 compared with met (+)-N. *P<0.05, **P<0.01, ***P<0.001, and ****P<0.0001 compared with met (+). #P<0.05, ##P<0.01, ###P<0.001, ####P<0.0001 compared to met (+) + 3-MA. ~P<0.05, ~~P<0.01, ~~~P<0.001, ~~~~P<0.0001 compared with met (-). &P<0.05, &&P<0.01, &&&P<0.001, &&&&P<0.0001 compared to met (-) + 3-MA.

[Downloaded from ijrr.com on 2026-08-16]

[DOI: 10.61186/ijrr.24.3.7]

DISCUSSION

In the methionine cycle [6], methionine is decomposed by methionine adenosyltransferase 2A (MAT2A) to form the methyl donor S-adenosyl-methionine (SAM). Methyltransferases (MTs) use SAM as the methyl source to produce S-adenosyl-homocysteine (SAH). SAH is converted to homocysteine (Hcy) by adenosyl-homocysteinase (AHCY), which then either participates in the transsulfuration pathway of glutathione (GSH) synthesis or contributes 5-methyl-tetrahydrofolate (5 -methyl-THF) in the folate cycle and is converted back to methionine-by-methionine synthetase (MS) with the aid of vitamin B12, thus completing the methionine cycle. In addition, methionine can be recovered from methylthioadenosine (MTA), a byproduct of polyamine metabolism via the methionine salvage pathway. Many types of cancer cells, such as glioma, melanoma, breast cancer, lung cancer, colon cancer and bladder cancer cells, are dependent on exogenous methionine. MD inhibits the proliferation of cancer cells, whereas normal cells, such as fibroblasts and liver, kidney and epithelial cells, can convert Hcy into methionine [16]. Therefore, the dependence of normal cells on exogenous methionine was lower than that of cancer cells. The dependence of cancer cells on methionine is defined as the inability of cancer cells to proliferate in methionine-deprivable medium even in the presence of Hcy [17]. Does MD have toxic effects on humans? An 18-week phase I clinical trial of MD in eight adults with various metastatic cancers reported a 58% decrease in plasma methionine within 2 weeks and an overall weight loss of approximately 0.5 kg per week. Data have shown that MD is relatively safe and tolerable in humans over a period of 18 weeks [18].

Liu *et al.* studied the effect of double deprivation of methionine and cystine (Cys) on the proliferation of glioma cells. The results revealed that the double deprivation of Met-Cys had a synergistic effect on increasing the level of reactive oxygen species (ROS), reducing the level of glutathione and inhibiting the proliferation of glioma cells [7]. In this study, we also found that MD inhibited the proliferation of glioma cells, especially under hypoxic conditions. It has been reported that MD induces apoptosis in prostate cancer cells but not in normal prostate epithelial cells [19]. Similarly, our results suggested that MD increased the degree of apoptosis in glioma cells induced by IR. Wang *et al.* reported that the MAT2A inhibitor FIDAS-539 and the S-adenosyl-homocysteine hydrolase (SAHH) inhibitor D9 weakened the colony formation and tumorigenesis ability of tumor-initiating cells (TICs) [20]. The results of our study revealed that MD weakened the colony formation ability of glioma cells and enhanced their radiosensitivity, even under hypoxic conditions. IR, especially low-LET radiation, damages biological macromolecules through active groups, such as free radicals, resulting in the production of ROS and reactive nitrogen species (RNS) [21], which in turn activate various signaling pathways, resulting in DNA damage, apoptosis and autophagy [22]. Paglin *et al.* reported that inhibition of the radiation-induced rapamycin-sensitive pathway led to an increase in autophagy in human breast cancer MCF-7 cells [23]. However, the results of Chaachouay *et al.* revealed that autophagy was beneficial for the ability of the radiation-resistant breast cancer cell line MDA-MB-231 to develop resistance to IR and that treatment with the autophagy inhibitors 3-MA significantly reduced the survival rate of irradiated cells [24]. In addition, Tseng *et al.* reported that IR-induced autophagy was radiation resistant in HepG2 cells, whereas 3-MA treatment inhibited the growth of tumor cells [25]. Therefore, radiation-induced autophagy has two distinct effects, protective or cytotoxic effects, the latter of which increase radiosensitivity. In this study, MD combined with an autophagy inhibitor significantly increased radiation-induced apoptosis and further increased the radiosensitivity of glioma cells.

ICD, also known as immunogenic apoptosis, is different from the general situation in which apoptosis is immune silenced. Some chemical and physical factors or virus infection can induce ICD through ROS and ERs, resulting in the release or exposure of DAMPs, thereby activating the antitumor immune response [26]. It has been reported that PERK -eukaryotic translation initiation factor 2 alpha (eIF2α) and/or IRE1-X-box binding protein 1 (XBP1) might constitute the main executive pathway of ERs after exposure to IR [27, 28]. Huang *et al.* reported that ionizing radiation induced ICD in a time-dependent manner. CRT exposure on the cancer cell membrane surface increased over time at 12, 24, and 48 h after proton, photon, and carbon ion irradiation, respectively [29]. Saglar *et al.* measured the expression of the glucose-regulated protein 78 (GRP78), ATF4, XBP1, growth arrest and DNA damage-inducible protein 153 (GADD153), autophagy-related 5 homolog (ATG5), and LC3 genes in peripheral blood samples from healthy volunteers irradiated with γ-rays and those from cancer patients receiving radiotherapy. The expression levels of these selected genes in both groups were increased, and the induction of ERs and autophagy in peripheral blood cells by IR was positively correlated with the dose of IR [30].

A study showed that autophagy promoted the release of ATP in the supernatants of mouse colon cancer CT26 cells and murine fibrosarcoma MCA205 cells, thereby activating dendritic cells (DCs) and cytotoxic T cells and improving cellular immune responses [31]. In contrast, Martins *et al.* demonstrated that autophagy had no effect on the surface exposure of CRT or the release of HMGB1 [32].

[Downloaded from ijrr.com on 2026-08-16]

[DOI: 10.61186/ijrr.24.3.7]

Our study revealed that MD promoted autophagy in glioma cells and increased cell membrane surface exposure of CRT and ATP release in the cell supernatant induced by IR. The reasons for these different results may be due to the different treatment conditions of MD and the different cell types.

In this study, we confirmed that MD inhibited proliferation, promoted apoptosis, aggravated DNA double-strand breaks and increased the radiosensitivity of normoxic or hypoxic glioma cells. MD combined with IR promoted autophagy. MD combined with 3-MA promoted apoptosis and further enhanced cell radiosensitivity. MD enhanced the ICD of normoxic or hypoxic glioma cells induced by IR through activating ERs signaling pathways. These results suggested that MD might be an effective way to radiosensitize glioma. However, a detailed characterization of the specific immune responses triggered by DAMPs release is lacking. Although increased release of DAMPs suggested a potential improvement in immune surveillance, a more thorough characterization of the immune effects following DAMPs release is essential. Further experiments are needed to evaluate downstream immune responses, such as enhanced DCs recruitment, *T-cell* activation and cytokine profiling following MD.

Acknowledgments: We thank Yanyan Li and Yufei Cao for excellent technical assistance and members of the Neurosurgery and Brain and Nerve Research Laboratory for their insights and discussion.

Author contributions: SY: collection and assembly of data, interpretation of findings, manuscript preparation. HQ, XJ, XX, HT and BW: methodology, validation. TS: experimental design, interpretation of findings. WY: experimental design, collection and assembly of data, interpretation of findings, manuscript preparation, supervision. AI was not used for manuscript preparation.

Funding: This work was supported by the National Natural Science Foundation of China (No. 32171234, 31870844, and 81874080), the State Key Laboratory of Radiation Medicine and Protection (GZK1202225 and GZK1202245), the Science and Technology Program of Suzhou (No. SKJY2021097), the Suzhou Fundamental Research Project (SJC2023001), the Key Laboratory of Radiation Damage and Treatment of Jiangsu Provincial Universities and Colleges and a project funded by the Priority Academic Program Development of Jiangsu Higher Education Institutions (PAPD).

Conflict of interest: No potential conflicts of interest were reported by the author(s).

Ethics approval: Not applicable.

REFERENCES

1. Ruan J, Qin Z, Chen P, Chen Y, Fang J, Tang H (2025) Paeonol combined with radiotherapy inhibits the growth of human glioblastoma by inhibiting the two angiogenesis pathways of VEGF/VEGFR and ANG/Tie-2 *in-vitro*. *Int J Radiat Res,* ***23****(3): 643-650*.
2. Zhu H, Luo J (2023) Postoperative intensity-modulated radiotherapy and chemotherapy in patients with high-grade glioma: analysis of efficacy and prognostic factors. *Int J Radiat Res,* ***21****(1): 139-145*.
3. Singh S, Dey D, Barik D, Mohapatra I, Kim S, Sharma M, *et al.* (2025) Glioblastoma at the crossroads: current understanding and future therapeutic horizons. *Signal Transduct Target Ther,* ***10****(1): 213*.
4. Nomura M, Spitzer A, Johnson KC, Garofano L, Nehar-Belaid D, Galili Darnell N, *et al.* (2025) The multilayered transcriptional architecture of glioblastoma ecosystems. *Nat Genet,* ***57****(5): 1155-1167*.
5. Qian J and Rankin EB (2019) Hypoxia-induced phenotypes that mediate tumor heterogeneity. *Adv Exp Med Biol,* ***1136****: 43-55*.
6. Sanderson SM, Gao X, Dai Z, Locasale JW (2019) Methionine metabolism in health and cancer: a nexus of diet and precision medicine. *Nature Reviews Cancer,* ***19****: 625-637*.
7. Liu H, Zhang W, Wang K, Wang X, Yin F, Li C, *et al.* (2015) Methionine and cystine double deprivation stress suppresses glioma proliferation via inducing ROS/autophagy. *Toxicol lett,* ***232****: 349-355*.
8. Gao X, Sanderson SM, Dai Z, Reid MA, Cooper DE, Lu M, *et al.* (2019) Dietary methionine links nutrition and metabolism to the efficacy of cancer therapies. *Nature,* ***572****: 397-401*.
9. Cao W, Li J, Yang K, Cao D (2021) An overview of autophagy: Mechanism, regulation and research progress. *Bull cancer,* ***108****: 304-322*.
10. Liu H, Xiao Y, Dai C, Chen K, Xu X, Cai J, *et al.* (2025) Research Advances of the Autophagy-Regulated Radiosensitivity. *Cell Prolif,* ***58****(10): e70056*.
11. Gui L, Chen K, Yan J, Chen P, Gao WQ, Ma B (2025) Targeting the mevalonate pathway potentiates NUAK1 inhibition-induced immunogenic cell death and antitumor immunity. *Cell Rep Med,* ***6 (2)****:101913*.
12. Garg AD, Krysko DV, Verfaillie T, Kaczmarek A, Ferreira GB, Marysael T, *et al.* (2012) A novel pathway combining calreticulin exposure and ATP secretion in immunogenic cancer cell death. *EMBO J,* ***31****: 1062-1079*.
13. Chen Y, Wang L, Chen N, Tang G (2024) Metformin induces tumor immunogenic cell death in ovarian cancer by activating AMPK pathway. *Transl Oncol,* ***47****: 102052*.
14. Scaffidi P, Misteli T, Bianchi ME (2002) Release of chromatin protein HMGB1 by necrotic cells triggers inflammation. *Nature,* ***418****: 191-195*.
15. Zheng L, Zhao Z, Chen L, Yang W, Ercolani G, Qin P, *et al.* (2025) Astragalin induces immunogenic cell death in liver cancer by targeting NQO2 to promote ROS-mediated endoplasmic reticulum stress pathway. *Free Radic Biol Med,* ***239****: 317-335.*
16. Yamamoto J, Han Q, Inubushi S, Sugisawa N, Hamada K, Nishino H, *et al.* (2020) Histone methylation status of H3K4me3 and H3K9me3 under methionine restriction is unstable in methionine-addicted cancer cells, but stable in normal cells. *Biochem Biophys Res Commun,* ***533****(4):1034-1038.*
17. Guéant JL, Oussalah A, Zgheib R, Siblini Y, Hsu SB, Namour F (2020) Genetic, epigenetic and genomic mechanisms of methionine dependency of cancer and tumor-initiating cells: What could we learn from folate and methionine cycles. *Biochimie,****173****: 123-128*.
18. Epner DE, Morrow S, Wilcox M, Houghton JL (2002) Nutrient intake and nutritional indexes in adults with metastatic cancer on a phase I clinical trial of dietary methionine restriction. *Nutr cancer,* ***42****: 158-166*.
19. Fu YM, Zhang H, Ding M, Li YQ, Fu X, Yu ZX, *et al.* (2006) Selective amino acid restriction targets mitochondria to induce apoptosis of androgen-independent prostate cancer cells. *J cell physiol,* ***209****: 522-534*.
20. Wang Z, Yip LY, Lee JHJ, Wu Z, Chew HY, Chong PKW, *et al.* (2019) Methionine is a metabolic dependency of tumor-initiating cells. *Nat med,* ***25****: 825-837*.

[Downloaded from ijrr.com on 2026-08-16]

[DOI: 10.61186/ijrr.24.3.7]

21. Jiajia D, Yiping W, Enyan J, Shouwu Z, Shuai Y, Xiaojian Z, *et al.* (2025) Maresin-1 alleviates lipid peroxidation-induced ferroptosis after radiation-induced brain injury in mice through the RORalpha/NRF2 pathway. *Exp Neurol,* ***389****:115258.*
22. Elkenawy NM, Ghaiad HR, Ibrahim SM, Aziz RK, Rashad E, Eraqi WA (2023) Ubiquinol preserves immune cells in gamma-irradiated rats: Role of autophagy and apoptosis in splenic tissue. *Int Immunopharmacol,* ***123****: 110647.*
23. Paglin S, Lee NY, Nakar C, Fitzgerald M, Plotkin J, Deuel B, Hackett N, McMahill M, Sphicas E, Lampen N, *et al.* (2005) Rapamycin-sensitive pathway regulates mitochondrial membrane potential, autophagy, and survival in irradiated MCF-7 cells. *Cancer Res,* ***65****: 11061-11070.*
24. Chaachouay H, Ohneseit P, Toulany M, Kehlbach R, Multhoff G, Rodemann HP (2011) Autophagy contributes to resistance of tumor cells to ionizing radiation. *Radiother oncol,* ***99****: 287-292.*
25. Tseng HC, Liu WS, Tyan YS, Chiang HC, Kuo WH, Chou FP (2011) Sensitizing effect of 3-methyladenine on radiation-induced cytotoxicity in radio-resistant HepG2 cells *in-vitro* and in tumor xenografts. *Chem biol interact,* ***192****: 201-208.*
26. Sun T, Li Y, Yang Y, Liu B, Cao Y, Yang W (2022) Enhanced radiation-induced immunogenic cell death activates chimeric antigen receptor T cells by targeting CD39 against glioblastoma. *Cell Death Dis,* ***13****(10): 875.*
27. Yang W, Xiu Z, He Y, Huang W, Li Y, Sun T (2020) Bip inhibition in glioma stem cells promotes radiation-induced immunogenic cell death. *Cell Death Dis,* ***11(9)****: 786.*
28. Xiu Z, Sun T, Yang Y, He Y, Yang S, Xue X, *et al.* (2022) Curcumin Enhanced Ionizing Radiation-Induced Immunogenic Cell Death in Glioma Cells through Endoplasmic Reticulum Stress Signaling Pathways. *Oxid Med Cell Longev,* ***2022****: 5424411.*
29. Huang Y, Dong Y, Zhao J, Zhang L, Kong L, Lu JJ (2019) Comparison of the effects of photon, proton and carbon-ion radiation on the ecto-calreticulin exposure in various tumor cell lines. *Ann Transl Med,* ***7****: 542.*
30. Saglar E, Unlu S, Babalioglu I, Gokce SC, Mergen H (2014) Assessment of ER stress and autophagy induced by ionizing radiation in both radiotherapy patients and *ex-vivo* irradiated samples. *J Biochem Mol Toxicol,* ***28****: 413-417.*
31. Michaud M, Martins I, Sukkurwala AQ, Adjemian S, Ma Y, Pellegatti P, *et al.* (2011) Autophagy-dependent anticancer immune responses induced by chemotherapeutic agents in mice. *Science,* ***334****: 1573-1577.*
32. Martins I, Michaud M, Sukkurwala AQ, Adjemian S, Ma Y, Shen S, *et al.* (2012) Premortem autophagy determines the immunogenicity of chemotherapy-induced cancer cell death. *Autophagy,* ***8****: 413-415.*

[Downloaded from ijrr.com on 2026-08-16]

[DOI: 10.61186/ijrr.24.3.7]

[DOI: 10.61186/ijrr.24.3.7] [Downloaded from ijrr.com on 2026-08-16]